International Journal of Heat and Mass Transfer 52 (2009) 5412–5422

Contents lists available at ScienceDirect

International Journal of Heat and Mass Transfer

journal homepage: www.elsevier.com/locate/ijhmt

Heating of saturated porous media in practice: Several causes of local thermal non-equilibrium ☆

L. Virto [a,*], M. Carbonell [b], R. Castilla [a], P.J. Gamez-Montero [a]

[a] Technical University of Catalonia, Department of Fluid Mechanics, Colom 7, 08222 Terrassa, Spain
[b] Technical University of Catalonia, Department of Fluid Mechanics, Av. Victor Balaguer s/n, 08800 Vilanova i la Geltru, Spain

ARTICLE INFO

Article history:
Received 2 May 2008
Accepted 9 July 2009
Available online 12 August 2009

Keywords:
Heating process
Porous media
Surfactant
Thermal conductivity

ABSTRACT

In recent years the industrial applications of porous materials has shown a growing relevance. Most of the technological thermal processes in porous media involve time-dependent thermal conditions. Therefore, the temperature at each point of the material also changes in time. In order to correctly carry out the technological process, it becomes necessary to know the temperature distribution inside the material. This is a problem of heat conduction in a fluid saturated porous media subject to a lack of local thermal equilibrium (LTNE).

The purpose of this paper is to elucidate the several causes of LTNE, even in steady or quasi steady heat transfer processes in saturated porous media, and to evaluate the influence of structural characteristic of porous media and the presence of surfactant in the saturating liquid phase.

1. Introduction

Many thermal processes require knowledge of thermal energy transport through porous media [1] such as biological systems [2], food processing [3,4], microheat exchanges [5], building insulation [6], nuclear reactor design and waste processing [7–9] and porous insert for thermal enhancement [10].

Most of heating processes in engineering are carried out putting the material in contact with a heat source. The heating of porous media by applying a heat source on the boundary is characterised by three different regimens:

(i) *Initial regimen or heating process beginning*. When the thermal perturbation at the boundary of porous medium is propagated-in.
(ii) *Intermediate regimen*. In this stage, the heat transfer rate decreases gradually becoming zero at the limit. The temperature variation rate strongly depends on the initial state. During this stage, the influence of initial irregularities disappears slowly and the temperature variation rate begins to become constant.
(iii) *Final stage*. After elapsing a large time (theoretically infinite), the steady state is attained, whose singular characteristic is the constant temperature distribution, provided that the temperature at the cold boundary is maintained constant by refrigeration.

Based on the traditional formulation of heat transfer in porous media, Vadasz [11] demonstrates that local thermal equilibrium applies generally for any boundary conditions that are a combination of constant temperature and insulation. But, in engineering practice, most of the heating processes are unsteady. Therefore, it can be expected that local thermal non-equilibrium (LTNE) exists because the pattern of heat flow within the solid phase of porous medium does not match within the fluid phase.

In relation to the lack of local thermal equilibrium there are many proposed criteria. Nield [12] shows that the "steady state" conduction for uniform thermal conductivities leads to LTE if the temperature, or its normal derivative on the boundary, is identical in both phases. Carbonell and Whittaker [13] performed a pioneering work on local thermal equilibrium. They presented a criterion for the validity of the assumption of local thermal equilibrium by using a magnitude order analysis in a representative elementary volume (REV) enclosing both the fluid and the solid phase.

Although many are the evidences of this LTNE behaviour [14–20], the assumption of LTE is very common, particularly in the study of reactions flows in porous media. However authors think that even if the criteria of validity proposed by Carbonell and Whittaker should be accomplished, there always are different

☆ Influence of structural characteristics of porous medium and the presence of surfactant in the liquid phase.

* Corresponding author. Tel.: +34 93 7886879; fax: +34 93 7398101.
E-mail address: virto13@telefonica.net (L. Virto).

0017-9310/$ - see front matter © 2009 Elsevier Ltd. All rights reserved.
doi:10.1016/j.ijheatmasstransfer.2009.07.003

Nomenclature

A	transversal section (m^2)
C	specific heat ($J\,kg^{-1}\,K^{-1}$)
$\bar{d}_p$	mean particle diameter (m)
h	porous media total height (m)
h_c	heat transfer coefficient ($W\,m^{-2}\,K^{-1}$)
K_f	thermal conductivity of fluid phase ($W\,m^{-1}\,K^{-1}$)
K_s	thermal conductivity of solid phase ($W\,m^{-1}\,K^{-1}$)
$\bar{L}$	mean length (m)
$\dot{q}$	heat flux ($W\,m^{-2}$)
S_e	specific surface (m^{-1})
T	temperature (K)
t	time (s)
$\dot{V}$	volumetric flux ($m^3\,s^{-1}$)
$W_{ac,i}$	accumulated heat in the porous medium (W)
$W_{rf,i}$	heat transfer per unit time to the refrigerating fluid (W)
$W_{tt,i}$	total heat transfer per unit time of the porous media (W)
z	position/axial coordinate (m)

Greek symbols

α	thermal diffusivity ($m^2\,s^{-1}$)
λ	thermal conductivity ($W\,m^{-1}\,K^{-1}$)
ν	kinematic viscosity ($m^2\,s^{-1}$)
Θ	dimensionless temperature: $\Theta = \frac{\langle T\rangle - T_0}{T_1 - T_0}$ where $\langle\rangle$ average
ρ	density ($kg\,m^{-3}$)
σ	surface tension ($mN\,m^{-1}$)
θ	temperature (°C)
ε	porosity
τ	relaxation time (s)

Subscripts

ac	accumulated
ef	effective
l	liquid phase
rf	refrigerating fluid
tt	Total
f	Function
s	solid
p	plate
c	contact

causes contributing to LTNE such as thermal boundary resistance (also called Kapitza resistance), solid surface wettability and lagging response.

1.1. Thermal boundary resistance (Kapitza resistance)

Kapitza found that when heat flowed between copper and superfluid helium a temperature step was developed at the interface and it was proportional to the heat flux [20,21].

The existence of the same phenomenon is known at every interface, even in a twin boundary of the same material, but it can be much stronger for an interface between two different materials [22–24].

Lloyd et al. [17] show that the contact resistance appears when the heat flux is applied to a saturated porous medium by a hot plate contacting it. In this case, the temperature distribution model assumes that sensible energy transferred from the interface plate–porous medium is deposited within a macroscopically thin boundary layer on the plate side.

1.2. Solid surface wettability

Near a solid–liquid boundary, spatially varying properties are prevalent and they have been correlated for the surface wettability [25].

Inside of porous media, if a non-condensing fluid (i.e. air) is occluded in the liquid phase, the dominating phase fills small size pores. The bulk of the large pores is occupied by less-wetting and non-wetting phase.

When two liquids are confined in micro-channels the relationship between wettability, the intensity of solid–liquid interaction and spatial variation of liquid properties is still valid. At the level of very small thickness of liquid–solid interface layer is quite hard to believe that thermodynamic equilibrium is reached because of the different basic heat conduction mechanism in either of the phases. Rah and Chan Eu [26] have developed a theoretical molecular equation for the thermal conductivity of liquids consisting in two parts: the first one given in terms of intermolecular forces structure and in terms of Chapman-Enskog thermal conductivity and the other one, in terms of the solids and the electron flux in the dominant heat conduction mechanism.

Efforts have been made to vary surface wettability in order to generate tailored transport properties within microscale solid–liquid systems. By using molecular dynamics Banat and Chiaruttini [27] demonstrated that tailored thermal resistance across a liquid–solid boundary can be obtained by tuning the strength of the solid–liquid interactions. The surface wettability is tuned by adjusting the solid–liquid parameter ε_{SL} in Lennard-Jones potential equations commonly used in molecular dynamics simulation of solid–liquid boundaries [28].

The addition of small amounts of soluble polymers makes the heat flux significantly higher for the same superheat at the heating surface [29].

All these solid–liquid interfaces makes that continuum based boundary conditions may not be applicable to microscale analysis. Then an understanding of the actual behaviour near surfaces and interfaces is required.

1.3. The lagging response

This behaviour in the transient process is caused by the finite time required for occurring structural interactions. When the heating of porous media is promoted by a hot plate, due to the presence of pores between the heater and the material volume, the heat flow produced by the hot plate at a general time t arrives at the material volume at a delayed time $t + \tau_q$. The internal pore within the material volume causes an additional delay in heat transport, prolonging the establishment of the temperature gradient at $t + \tau_T$.

This type of delayed response depends on the detailed configuration of the solid particles and the interstitial gas within the material volume. The two phase lags τ_T and τ_q, like the thermal diffusivity and thermal conductivity, are intrinsic thermal properties of the bulk material. In porous media, they become "structural properties", which also depend on the detailed configuration of the structures.

In the classical theory of diffusion, the heat flux vector $\vec{q}$ and the temperature gradient ∇T across a material volume are assumed to occur at the same instant of time. In the wave theory of heat conduction, on the other hand, the heat flux vector and the temperature gradient across a material volume are assumed that will occur at different instants of time. Assuming an instantaneous

heat flow, the time delay, called the "relaxation time" is defined by the wave model formulated by Cattaneo and Vernotte [30–32].

In applications that involve short time thermal perturbation of porous media [33], subjected to a rapidly changing heat source, different temperature may exist between solid and fluid. Hence the two equations of heat transfer [18,34] are not coupled and can no longer be reduced to a single equation for $(T_s - T_f)$.

Tzon et al. [35] developed a procedure for the determination of τ_T in the case of a porous medium heated at the boundary with a heat flux $\vec{q}$ by knowing the thermal conductivity λ. They use the linear version of the energy equation and the constitutive equation based on the first order expansion of τ_T and τ_q. Then, they obtained the phase lag of the temperature gradient τ_T from the initial slope of the T vs. t curve recorded at the heated end.

2. Experimental studies

In order to show the possible causes of local thermal non-equilibrium in the engineering practice of heating saturated porous media, authors have carried out some heating experiences under thermal conditions that can be bound in industrial common applications.

2.1. Porous media tested

The porous media that have been studied are the following:

- Bronze powder saturated by water and by a solution of surfactant, hereinafter referred to as *Bronze + W* and *Bronze + DS*, respectively. Geometrical porosity: 0.36.
- Sand saturated by water and by a solution of surfactant, hereinafter referred to as *Sand + W* and *Sand + DS*, respectively. Geometrical porosity: 0.38.
- Cotton fibre saturated by water and by a solution of surfactant, hereinafter referred to as *Cotton + W* and *Cotton + DS*, respectively. Geometrical porosity: 0.83.

These three porous media have very different chemical natures of solid phase (metallic, mineral and organic), different thermophysical properties of both phases, different transport properties (viscosity and surface energy) of liquid phase and different geometrical characteristics of solid components. They have been selected in order to verify the influence of the nature of the solid phase, transport properties of the liquid phase and their structural characteristic (porosity, specific surface area, etc.) on the thermal response of the porous medium submitted to an unsteady heating process.

Geometrical characteristics (shape, size and specific surface area) and thermophysical properties of the solid matrix elements of the previous mentioned porous media are shown in Table 1.

With regard to the saturating liquid phase, Table 2 shows a summary of values of the most important properties. The solution of surfactant is obtained by adding distilled water 0.8 g/l of Nonilfenol 30-0E, a non-ionic active agent.

The porous media are submitted to an unsteady heating process by applying a heat flux, on one boundary through a hot plate, and maintaining a constant temperature at the other boundary by refrigeration. The thermal response of porous media under these thermal boundary conditions is obtained by measuring the temperature at several interior points (minute by minute) and the incremental temperature of refrigerating water flow.

Fig. 1 shows the experimental equipment which is constituted by a cell formed by a cylinder of stainless steel in which the porous medium is compacted. The base of the cell is a stainless steel plate of 0.5 m gauge, which is part of the refrigerating chamber where water circulates. The cell is closed with an aluminium plate pressing the porous medium. This plate has incorporated an electric resistance heater which is connected to an adjustable current transformer. The temperature is measured by using thermocouples placed within the porous medium at different distance from the heating plate. The electrical signal is automatically registered by a data acquisition system.

The heat flow transferred to the water at the refrigerating chamber is calculated by measuring the water flow rate and its increment of temperature through thermocouples.

3. Experimental results

The experimental results concerning to the field of temperatures inside the porous medium are represented by the surface $T = T(z,t)$ of in Fig. 2(a)–(h). A function which fits the surface of state with a $r^2 > 0.9$ is as follows:

$$\ln T = a + bt^{0.5} + \frac{cz}{\ln z} \tag{1}$$

which reveals the dependence of the temperature T with $\sqrt{t}$ and z. Fig. 3 shows, as an example, the heat power transferred vs. time, to the refrigerating water flow by the Bronze + W and Bronze + DS porous media.

Other representations can be brought out from the previous figures, such as that show the temperature variation vs. time, by taking the position as a parameter. For instance, Fig. 4, for Bronze + W and Bronze + DS, respectively. In all the cases, the fitting equations $T_i = T_i(t)$, $T_j = T_j(z)$, $i,j = 1,2,\ldots,5$ have been obtained by using the least square method and maximum value of r^2, usually of 0.9999 order.

Table 1
Geometrical characteristics and thermophysical properties of the solid phase.

Solid phase	Mean diameter $d_p \times 10^{-4}$ (m)	Mean length $L \times 10^{-3}$ (m)	Density ρ (kg m^{-3})	Specific surface S_e (m^{-1})	Specific heat C (J kg^{-1} K^{-1}) at 20 °C	Thermal conductivity λ (J s^{-1} m^{-1} K^{-1}) at 20 °C
Bronze	2.355	–	8614.05	25477.7	376.00	71.00
Sand	29.60	–	2613.95	2027.0	527.90	31.39×10^{-2}
Cotton	0.145	11.35	1176.25	274819.7	1329.98	5.89×10^{-2}

Table 2
Thermophysical properties of the saturating liquid phase.

Liquid phase	Density ρ (kg m^{-3}) at 20 °C	Cinematic viscosity ν (m^2 s^{-1}) at 20 °C	Specific heat C (J kg^{-1} K^{-1}) at 20 °C	Thermal conductivity λ (J s^{-1} m^{-1} K^{-1}) at 20 °C	Surface tension σ (mN m^{-1})
Distilled water	998.2	1.01×10^{-6}	4182.8	0.598	75.83–0.1477 T (°C)
Diluted solution	998.2	0.96×10^{-6}	4182.8	0.598	46.42–0.1312 T (°C)

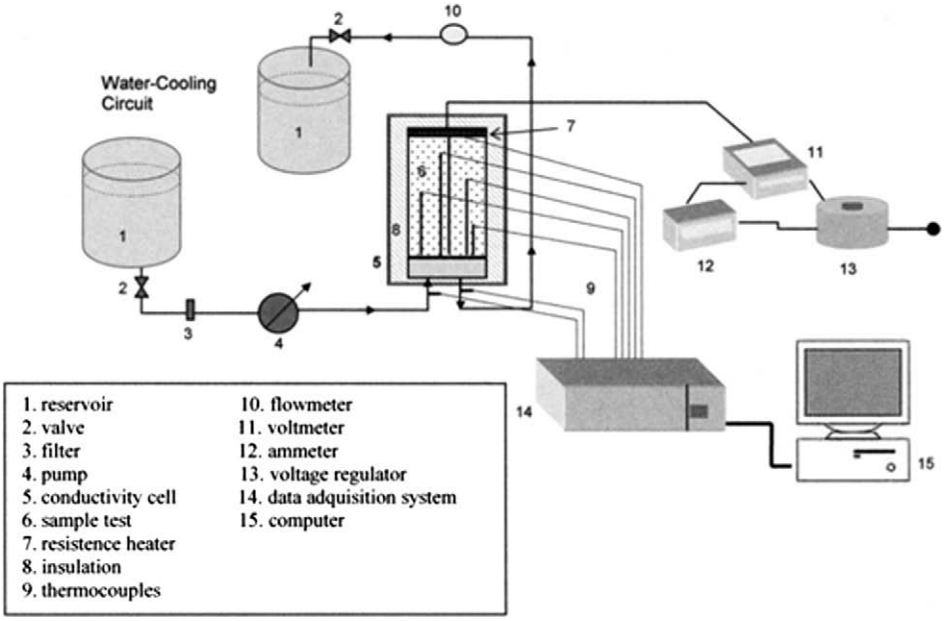

Fig. 1. Experimental equipment scheme.

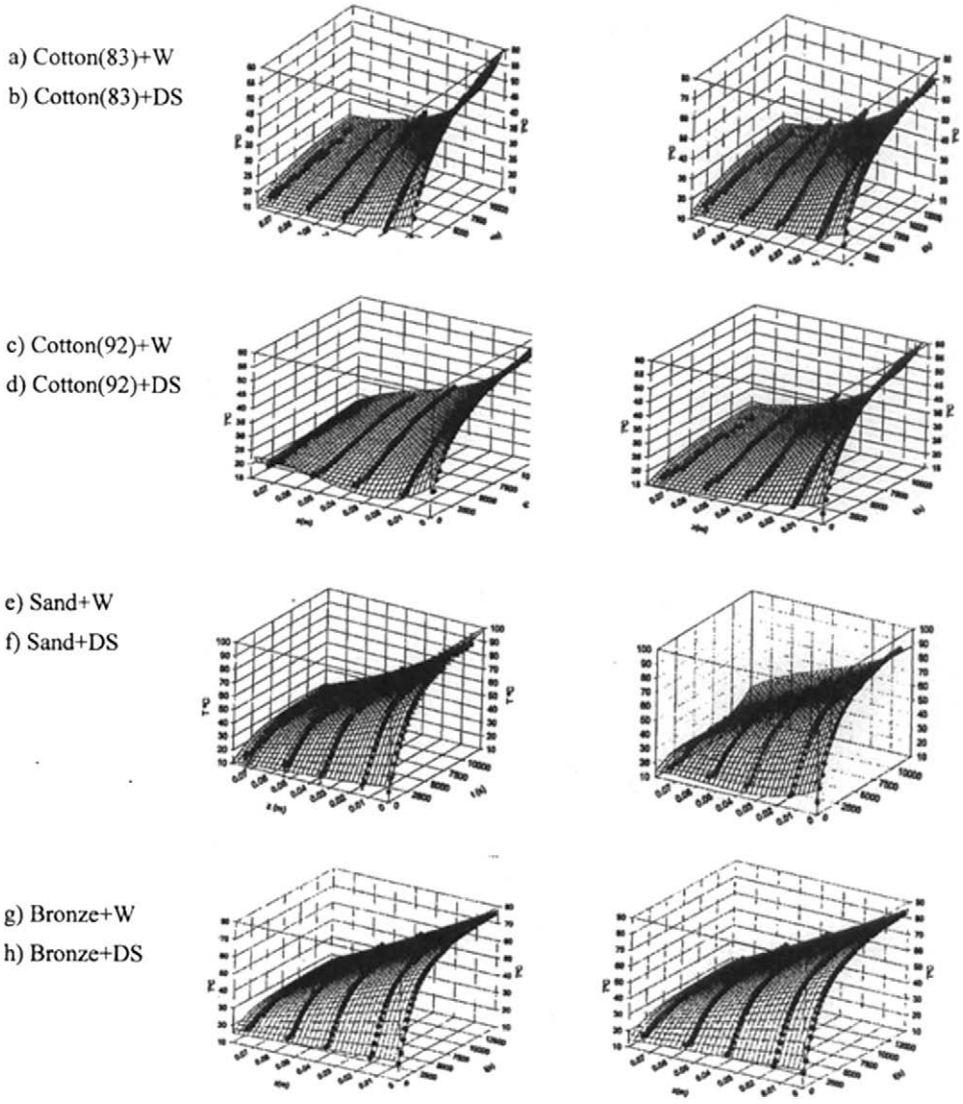

Fig. 2. Surface of state $T = T(z,t)$ of the different porous media.

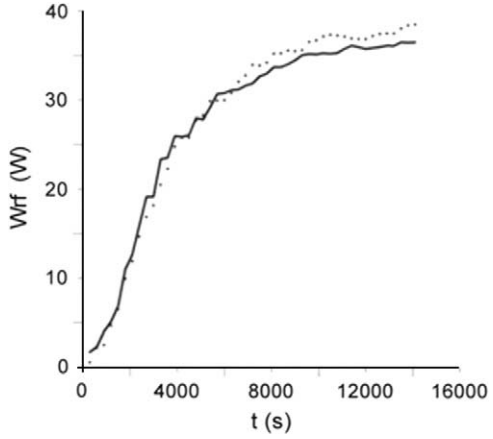

Fig. 3. Curves W_{rf} vs. t to the porous media Bronze + W (continuous line) and Bronze + DS (dotted line).

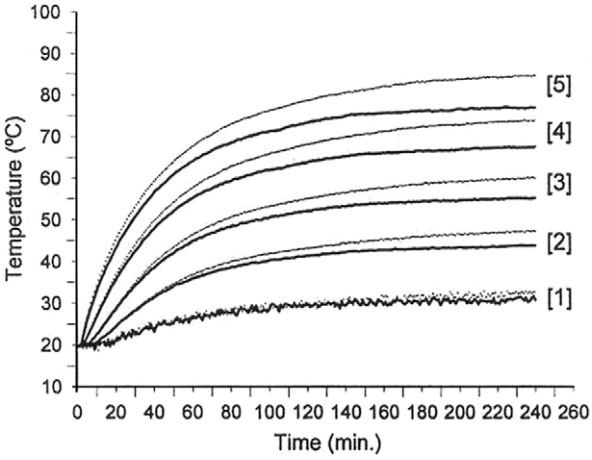

Fig. 4. Temperature distribution vs. time at the corresponding thermocouples locations to Bronze + W (continuous line) and Bronze + DS (dotted line), respectively. [ ] Thermocouples.

From the fitting equations $T_i = T_i(t)$ and $T_j = T_j(z)$, with corresponding derivative $\partial T_i/\partial t$ and $\partial T_j/\partial z$, have been calculated. Now, values of T vs. z, t and its corresponding derivatives are available. The value of other characteristic magnitudes to unsteady heating process of porous media tested can be now determined through the most reliable methods and with the expected accuracy to its application. Among them, it has been carried out the following ones:

1. *Temporal temperature variation in five different locations inside the porous media.* T_5 at interface hot plate–porous medium $z = 0$; T_4 at 13.75 mm from the hot plate; T_3, T_2 and T_1 at 35.18, 53.78 and 73.48 mm from the hot plate, respectively. Results are plotted in Fig. 4.
2. *Spatial temperature variation inside the porous media at different times of the heating process.* Results are plotted in Fig. 5a and b.
3. *The accumulated heat per second*, W_{ac}, at the porous medium vs. time: $W_{ac,i} = \langle \rho C_p \rangle_i, A \int^h \left(\frac{\partial T}{\partial t}\right) dz$. Results are plotted in Fig. 6.

From all these results it can be calculated the thermal conductivity and diffusivity of porous media under conditions near to the steady heat transfer and the time parameter of lagging response of unsteady heating process. Also, it can be evaluated the influence of dilute solution of surfactant as saturating liquid of porous media upon their thermal properties.

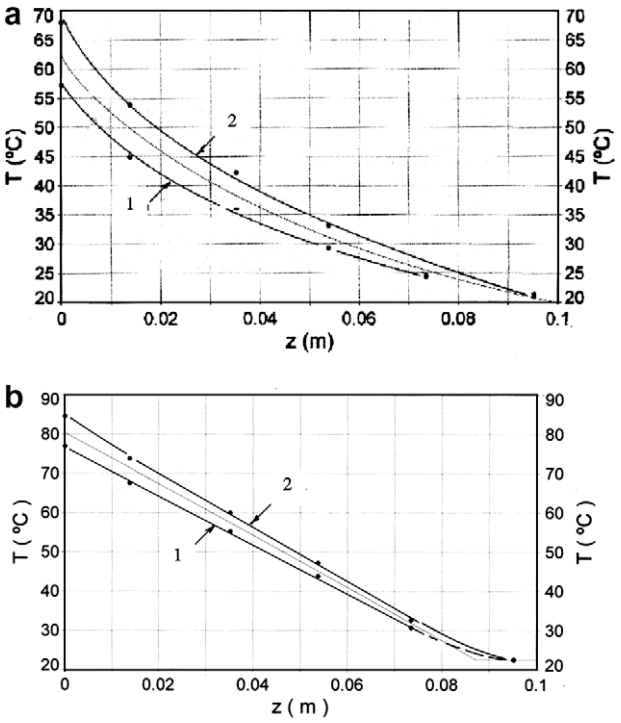

Fig. 5. (a) (1) Cotton 83 + W and (2) Cotton 83 + DS, (b) (1) Bronze + W and (2) Bronze + DS.

3.1. Thermal conductivity and diffusivity

In these experiences, the steady state is never reached. At the end of heating process, the temperature variation rate of the porous media is about 1.18×10^{-4} °C/s for Bronze + W, 2.92×10^{-4} °C/s for Sand + W and 5.78×10^{-4} °C/s for Cotton 83 + W. However, these temperature rate values are small enough to allow the thermal conductivity applying Fourier law or the Price's method. W.L. Price puts forward a method to calculate the thermal conductivity and thermal diffusivity from measurement at non-stationary heat conduction. The method lays on the contribution of a heat flux $\dot{q}$ to the porous medium through a heating plate. At the same time, the porous medium is maintained at constant refrigerating temperature T_{rf} through a parallel surfaces separated from the heating plate. The difference in temperature θ vs. time t between layers, which are separated a distance z of the porous medium from the initial moment of application of heat flux, is obtained by,

$$\theta = \frac{\dot{q}z}{K_{ef}}\left[1 - \frac{8}{\pi^2}\sum_{n=0}^{\infty}(2n+1)^{-2}, \exp\left\{-\frac{(2n+1)\pi^2\alpha_{ef}t}{4z^2}\right\}\right] \tag{2}$$

After some transformations,

$$\theta = \frac{\dot{q}z}{K_{ef}} - \left(\frac{4z^2}{\pi^2\alpha_{ef}}\right)S \tag{3}$$

where S denotes $d\theta/dt$.

Eq. (2) is physically represented at the co-ordinate (θ, S) by a straight line, with the ordinate at the origin $\dot{q}z/K_{ef}$ and the slope $-(4z^2/\pi^2\alpha_{ef})$. Then, K_{ef} and α_{ef} can be calculated. On the other hand, if the Fourier law can be applied,

$$K_{ef} = \frac{\dot{q}z}{\nabla T} \quad \text{and} \quad \alpha_{ef} = \frac{K_{ef}}{(\rho C_p)}$$

where $\langle \rho C_p \rangle = \varepsilon(\rho C_p)_f + (1-\varepsilon)(\rho C_p)_s$.

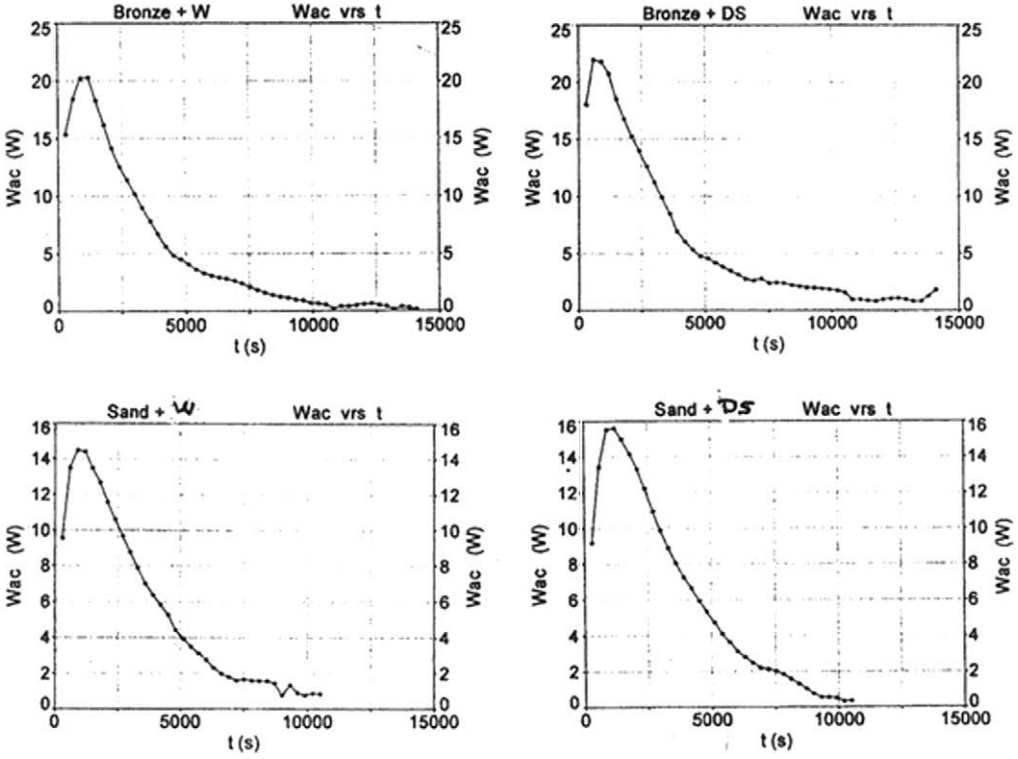

Fig. 6. Accumulated heat by second, W_{ac}, in the porous medium.

Fig. 7(a)–(d) shows the results (θ,S) obtained applying the Price's method to Sand + W, Sand + DS, Bronze + W and Bronze + DS porous medium.

Table 3 resumes the corresponding calculated values of K_{ef} and α_{ef}. Table 4 summarises the results obtained applying the Fourier's law at the end of the heating process. The corresponding values of

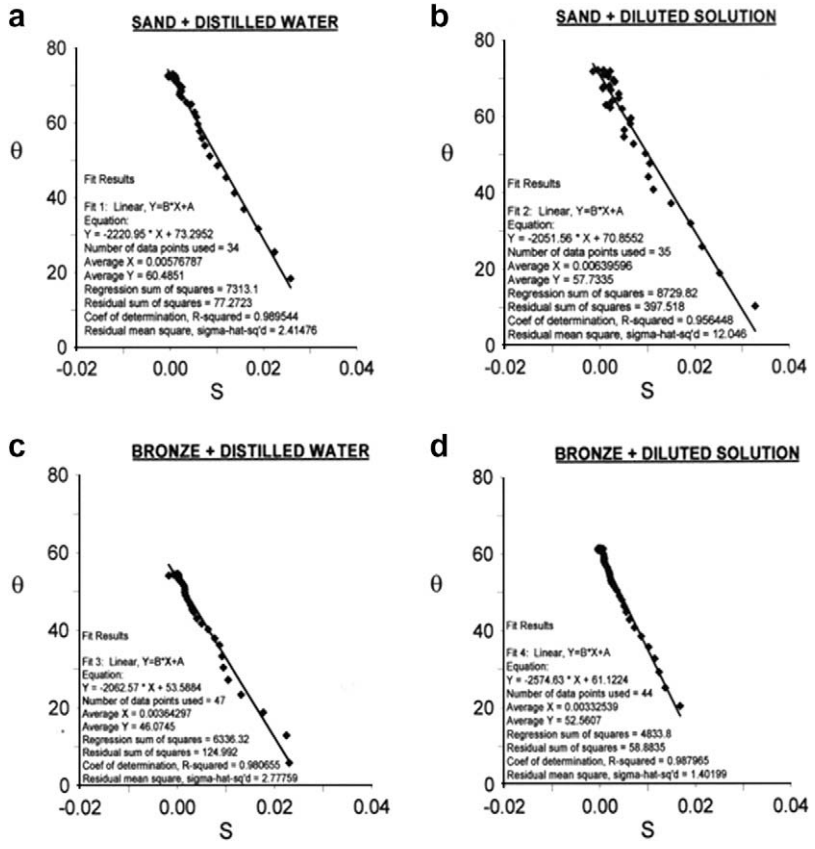

Fig. 7. a (top-left), b (top-right), c (down-left), d (down-right). Least squares fitting lines of the experimental values (Θ,S).

Table 3
Values of K_{ef} and α_{ef}.

	t (seg)	$\dot{q}$(W m^{-2})	z (m)	$\theta_{s=0}$	$d\theta/ds$	K_{ef} (W m^{-1} K^{-1})	α_{ef} (m^2 s^{-1})
Sand + W	10,800	2823.17	0.0952	73.295	−2220.95	3.667	1.65385×10^{-6}
Sand + DS	10,800	1742.42	0.0952	70.855	−2051.56	2.341	1.7904×10^{-6}
Bronze + W	14,400	4894.23	0.0952	53.588	−2062.57	8.695	1.7808×10^{-6}
Bronze + DS	14,400	4812.48	0.0952	61.122	−2574.83	7.496	1.4262×10^{-6}

Table 4
Fourier's law at the end of the heating process.

	t (seg)	$10^6\dot{V}$ (m^3 s^{-1})	ΔT_{rf} (°C)	$\dot{q}$ (W m^{-2})	∇T (°C m^{-1})	K_{ef} (W m^{-1} K^{-1})
Cotton + W	10,800	3.735	0.5168	1026.09	−405.59	2.531
Cotton + DS	10,800	3.672	0.5667	1107.39	−517.20	2.142
Sand + W	10,800	3.167	1.676	2823.17	−777.13	3.633
Sand + DS	10,800	3.276	1.2346	1742.42	−792.49	2.198
Bronze + W	14,400	4.116	2.2356	4894.23	−615.77	7.948
Bronze + DS	14,400	4.187	2.1610	4812.48	−689.06	6.984

α_{ef} are obtained as $K_{ef}/\langle\rho C_p\rangle$. Table 5 summarises the values of $\langle\rho C_p\rangle$ and α_{ef}.

4. Approaching models of temperature field inside the porous media

The heating process in these experiences is quite complex. In fact, authors would like to reproduce the most frequent conditions that can be found in the engineering practice: heat flux source intensity rising in time, constant temperature at the cold end, with or without heat transfer in it.

The experiences show that the heat transfer at the hot and cold boundaries, is non-Fourier, as Fig. 8 shows the temperature field in Sand + W porous medium after 3600 s from the beginning of the process. It seems obvious that at the two boundary locations $x = 0$ and $x = 0.0952$, the heat flow is defined by a heat transfer coefficient, h_c, function of the interface contact. Fig. 8 also shows the temperature field in Bronze + W porous medium after 14,400 s from the beginning of the process.

An approach model that could be used to calculate $h_c = h_c(0,t)$ in order to compare both modelling and experimental results and agents in the saturating liquid, is the following:

$$K_{ef}\frac{\partial T}{\partial z} + h_c(T_p - T) = 0$$
$$\text{where in } z = 0 \rightarrow T = T_0 = T_p \text{ to } t = 0 \text{ and } \forall z$$
$$\dot{q} = h_c(T_p - T) \tag{4}$$

where T_p is the hot plate temperature when the heat flux to porous medium is $\dot{q}$. If it is taken $= T_p - T + \frac{K_{ef}}{h_c}\frac{\partial T}{\partial z}$, then the Fourier's equation is written as:

$$\frac{\partial f}{\partial t} = \alpha\frac{\partial^2 y}{\partial z^2} \tag{5}$$

Now, the boundary conditions are $f = T_p$ when $t = 0$; $f = 0$ in $z = 0$. The solution of Eq. (5) is,

$$f(z,t) = \frac{2T_p}{\sqrt{\pi}}\int_0^{\frac{z}{z\sqrt{\alpha t}}} e^{-\mu^2}d\mu \tag{6}$$

In order to evaluate T,

$$K_{ef}\frac{\partial T}{\partial z} + h_c(T_p - T) = -f(z,t)\cdot h_c \tag{7}$$

After integration, the solution obtained is as follows,

$$\frac{T}{T_p} = \text{erf}\left\{\frac{z}{2\sqrt{\alpha t}}\right\} + \exp\left\{\frac{hz + h_0^2\alpha t}{K_{ef}}\right\}\text{erfc}\left\{\frac{z}{2\sqrt{\alpha t}} + \frac{h_c}{K_{ef}}\sqrt{\alpha t}\right\} \tag{8}$$

From this equation, h_c can be calculated by knowing α and K_{ef}. The values of T can be taken from the corresponding experience for all $z > 0$, $t > 0$. Once h_c is calculated, the values of T can be known from Eq. (4) for all $t > 0$. Then, by taking this temporal distribution of the temperature as a boundary condition, $T(z,t)$ can be calculated by applying a Fourier's model.

In order to obtain the order of magnitude of h_c, Eq. (8) can be simplified considering that,

$$\text{erfc}\left\{\frac{z}{2\sqrt{\alpha r}} + \frac{h_c}{K_{ef}}\sqrt{\alpha t}\right\} \sim 0(1) \quad \text{and} \quad \text{erf}\left\{\frac{z}{2\sqrt{\alpha t}}\right\} \sim 0(1)$$

Then,

$$\frac{T}{T_p} \sim 0\left[\exp\left\{\frac{hz + h_c^2\alpha t}{K_{ef}}\right\}\right]$$

For instance, in $z = 0.01375$ m from the hot plate at $t = 600$ s the temperatures measured are $T_p = 36.715$ °C and $T(z) = 24.973$ °C, obtaining $h_c \cong 34$ W/m^2 K, approximately. In order to compare experimental and theoretical results, the classical model of semi-infinite body heating can be used, initially with an uniform temperature T_t when the surface temperature variation is specified as a prescribed function $f(t)$ for $t \geqslant 0$ [36].

The formulation of the problem in terms of $\theta(z,t) = T(z,t) - T_i$ assuming constant thermophysical properties, is given by,

Table 5
Values of $\langle\rho C_p\rangle$ and α_{ef}.

	ε	ρ_f (kg m^{-3})	ρ_s (kg m^{-3})	c_{pf} (J kg^{-1} K^{-1})	c_{ps} (J kg^{-1} K^{-1})	$\langle\rho C_p\rangle$	$10^6\alpha_{ef}$ (m^2 s^{-1}) W	$10^6\alpha_{ef}$ (m^2 s^{-1}) DS
Cotton + W + DS	0.83	948.2	1176.25	4182.8	1329.91	3731421.0	0.6782	0.57
Sand + W + DS	0.38	948.2	2613.95	4182.8	527.9	2442143.6	1.4876	0.9
Bronze + W + DS	0.36	948.2	8614.05	4182.8	376	3575982.5	2.2226	1.953

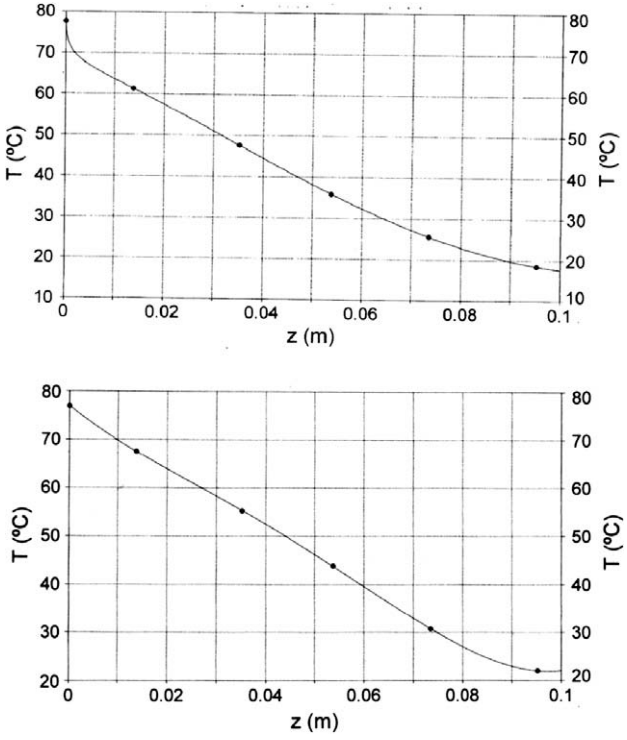

Fig. 8. Sand + DS; t = 3600 s; $T^2 \cong 1$ (up), Bronze + W; t = 14,400 s (down).

$$\frac{\partial^2\theta}{\partial z^2} = \frac{1}{\alpha}\frac{\partial\theta}{\partial t}; \quad \theta(z,0) = 0; \quad \theta(0,t) = f(t) - T_i; \quad \lim_{z\to\infty}\theta(z,t) = 0$$

The solution is,

$$T(z,t) = T_i - T_i\mathrm{erfc}\left\{\frac{z}{2\sqrt{\alpha t}}\right\} + \frac{z}{2\sqrt{\pi\alpha}}\int_0^t \frac{(t-t')}{(t')^{\frac{3}{2}}}\exp\left(-\frac{z^2}{4\alpha t'}\right)dt'$$

That can be rewritten as,

$$T(z,t) = T_i\mathrm{erfc}\left\{\frac{z}{2\sqrt{\alpha t}}\right\} + \sum_{i=1}^{n}[f(\tau_i) - f(\tau_{i-1})]\mathrm{erfc}\left\{\frac{z}{2\sqrt{\alpha(t-\tau_i)}}\right\} \quad (9)$$

For instance, at t = 2400 s the temperature measured at z = 0.01375 m is 48.426 °C, and the one calculated by using time intervals $\Delta\tau = \tau_i - \tau_{i-1}$ = 60 s is 49.02 °C.

On the other hand, from the known values of α_{ef} and K_{ef} obtained experimentally it can be calculated the values of h_c for all t in z = 0, applying Eq. (8). Then, it can also be calculated the values of $T(z,t)$. For instance, for the Sand + W porous medium at z = 0 and z = 0.01375 m the temperature values measured after 5400 s from the beginning of the heating process are:

$$T_{p,exp} = 87.34\,^\circ\mathrm{C}, \quad T = 70.375\,^\circ\mathrm{C}$$

$$\left(\frac{T}{T_p}\right)_{exp}(z=0, t=5400\,s) = 1 \rightarrow h \cong 6\,\mathrm{W/m^2\,K}; T(\mathrm{Eq.\ (8)}) = 75.15\,^\circ\mathrm{C}$$

The temperature gradient value at the same (z,t) is −688.47 °C/m. Applying Fourier's law, it gives $T_{p,F} \cong 79.53\,^\circ\mathrm{C} \ll T_{p,exp}$. This comparative shows the influence of thermal contact conductance at the interface heating plate–porous medium.

5. Critical analysis of experimental results

Basically, experimental results show that the heating process cannot be modelled assuming local thermal equilibrium. Despite of the slow temperature rising at the heating plate, the contact conductance at the two interface plate–porous medium, at hot and cold ends, where the heat flow is non-Fourier, are very important perturbation causes. Therefore, it can be drawn out several conclusions.

5.1. Thermal conductivity and diffusivity

The values of thermal conductivity and thermal diffusivity calculated by using Price's method (applied to overall experimental results) and Fourier's law (applied only to the results at the last time of the heating process) are nearly the same. The maximum difference between the two values corresponding to the Bronce + W, attains about 8%. However, this difference is more important when confronts the values corresponding to the same porous media saturated by water and saturated by dilute solution of surfactant. The maximum occurs in the porous media with solid matrix of sand, attaining about 40%. The presence of surfactant diminishes the bulk thermal conductivity coefficient as well as the bulk thermal diffusivity in all the porous media tested. This effect can be due to adsorption of surfactant on the solid surface. Fig. 9 shows the uptake isotherm absorption of the non-ionic surfactant on quartz sand [37] from aqueous solution, where $\Gamma = \frac{(c_0 - c_{eq})V}{mS_{sp}}$ is the uptake.

The wetting angle for quartz sand is zero, indicating the formation of a strong wetting film of aqueous solution of surfactant on the sand surface, with a specific surface of $S_{sp} \cong 0.03\ \mathrm{m^2/g}$. This film does not break when an air bubble is brought into it. The main effect of this film is to increase the solid surface in contact to the liquid solution by wetting, so that the heat transfer from liquid to solid phase is enhanced. Fig. 10 shows how increases the heat

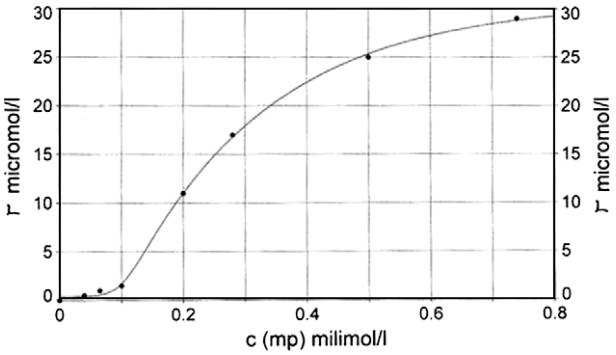

Fig. 9. Uptake isotherm absorption of the non-ionic surfactant on quartz sand from aqueous solution.

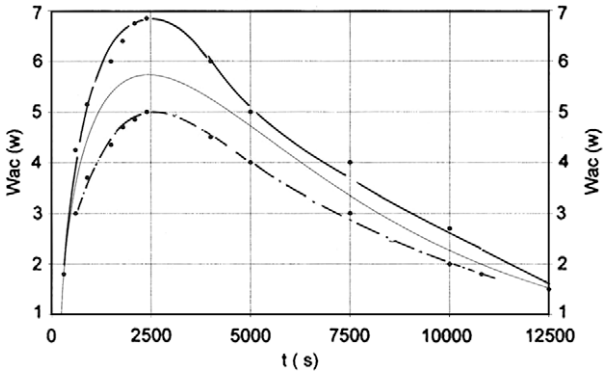

Fig. 10. Cotton 83 + DS (continuous line) and Cotton 83 + W (dash line).

accumulated in solid phase of porous media and their heating rate when the saturating liquid phase is the surfactant solution [38].

5.2. Heat transfer at the boundary hot plate–porous medium

The coupling of the bounding surface thermal conductivity and the effective thermal conductivity of the porous medium on and near to the bounding solid surface is a very complex problem. The application at the interface of the bulk value of effective thermal conductivity can lead to significant errors in the predicted heat flow rate. The factors contributing to the difference between the two thermal conductivities are the non-uniformity porosity, the contact area between the elements of matrix and the boundary surface, and the location of the interface.

Assuming that the local effective thermal conductivity is uniform over a distance $d/2$ from the surface, Ofuchi and Kunii [39] have proposed an empirical relation for the local effective thermal conductivity. However, the expression is valid only for a loose packing of monosize spherical particles.

From the experimental results it seems that the ratio of surface boundary fraction in contact with the liquid phase and with the solid phase of porous medium is a function of the bulk porosity, form and size of the solid matrix elements. Besides, the wetting degree of the boundary surface must have some influence on thermal conductivity.

Applying Fourier's law to a layer of porous medium separated a distance greater enough than $d/2$ from the heating surface, knowing the heat flux and calculating the temperature gradient, the bulk thermal conductivity coefficient values have been obtained. The values are shown in Table 6 where K_{ec} is the bulk thermal conductivity coefficient at $z = d/2$, and K_{eb} is the bulk thermal conductivity coefficient of porous medium assuming that Fourier's law can be applied. K_{ec}/K_{eb} values show the influence of plate–porous medium contact. This influence is as greater than lesser is the thermal conductivity of solid matrix in porous medium.

5.3. The lagging response

The unsteady heating process is characterised by a temperature variation rate in all points inside the porous medium. This temperature variation and heat flux $\vec{q}$ are taken into account writing the energy equation in the form [33],

$$\vec{q}(\vec{r}_i t + \tau_q) = -K\nabla T(\vec{r}_i t + \tau_r)$$

No general solution has yet been found for this type of equation when delays are considered. For the advancement of the dual phase-lag model, the thermal conductivity and the thermal diffusivity must be determined experimentally. Although the boundary condition of constant heat flux experiences is not exactly achieved, we can use this method for determining the lag time of heat flux. By plotting $\vec{q}$ vs. t, the slop of the q–t curve at $t = 0$ is clearly,

$$\left(\frac{\partial \vec{q}}{\partial t}\right)\Big|_{t=0} = -\left\{\frac{K\nabla T}{\tau_q}\right\}$$

From the q vs. T values calculated for the Bronze + DS porous medium, Fig. 11, it is obtained,

Table 6
Bulk thermal conductivity coefficient values.

Cotton		Sand		Bronze		
+W	+DS	+W	+DS	+W	+DS	
0.6388	0.6234	1.3758	0.799	5.469	4.5877	W m^{-1} K^{-1}
0.2524	0.29	0.3787	0.3635	0.6881	0.6569	K_{ec}/K_{eb}

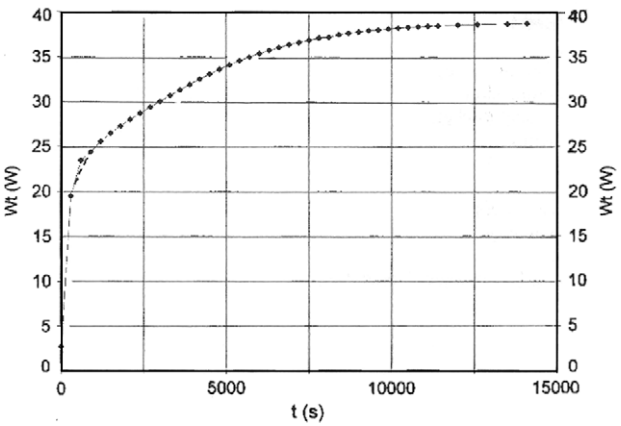

Fig. 11. Bronze + DS.

$$\left(\frac{\partial \vec{q}}{\partial t}\right)\Big|_{t=0} = 12.936\ \mathrm{W/m^2\ s}; \quad |K\nabla T| = 4933.8\ \mathrm{W/m^2}$$

and hence, $\tau_q = 381.1$ s.

For the same porous medium, the lag time of temperature gradient is calculated by using the equation:

$$\frac{\partial \Gamma}{\partial t}\Big|_{x=0,t=0} = -\frac{qL}{K\tau_T}$$

From the curve T vs. t the calculated value of $\frac{\partial \Gamma}{\partial t}$ at $x = 0$, $t = 0$ is 0.0138965 °C/s, and $\tau_T = 4253.9$ s. For the Bronze + W porous medium, the phase lag of temperature gradient is calculated from the value $\frac{\partial T}{\partial t} = 0.0113$ °C/s at $x = 0$, $t = 0$, and hence $\tau_T = 4741.9$ s.

It can be concluded that when the porous media are submitted to time thermal perturbation, even for long time temperature variation processes, heat conductivity behaviour is definitely non-Fourier. In these cases, the governing energy equation is formulated based on the two-equation model. This formulation essentially leads to emergence of two thermal lag times which take into account the thermal interaction between the fluid and the solid phases of porous media as well as the delayed time for both phases to approach thermal equilibrium.

5.4. Isotherm front propagation

If a isotherm front propagation is promoted by a plane wave $T = \theta(z - vt)$, then it necessarily satisfies $-\rho c v\frac{d\theta}{dz} = \frac{d}{dz}\left(k\frac{d\theta}{dz}\right)$. Introducing this velocity in the diffusion equation $\frac{\partial T}{\partial t} = \alpha\frac{\partial^2 T}{\partial z^2}$, it is obtained: $-\frac{v}{\alpha} = \frac{d}{dz}\left(\ln\frac{d\theta}{dz}\right)$.

Integrating: $-\frac{vz}{\alpha} + C_1 = \ln\left(\frac{d\theta}{dz}\right)$.

At $z = 0 \Rightarrow C_1 = \ln\left(\frac{d\theta}{dz}\right)_{z=0}$, and hence: $v = \frac{\alpha}{z}\ln\left\{\frac{(d\theta/dz)_{z=0}}{(d\theta/dz)}\right\}$.

Fig. 13 shows the front position vs. time for different isotherm temperature in the porous media Bronze + W and Bronze + DS. The isotherm front propagation velocity is given by the curve slope in each point, and it is diminishing as the distance to the hot plate increases.

6. Conclusions

From the experimental results obtained it can be drawn the following conclusions:

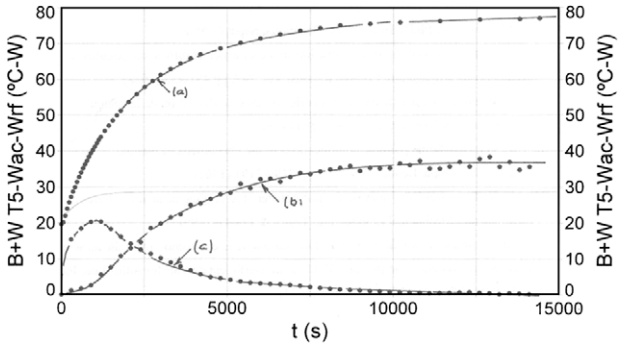

Fig. 12. (a) $T_p(t)$, (b) $W_{rf}(t)$, $W_{ac}(t)$.

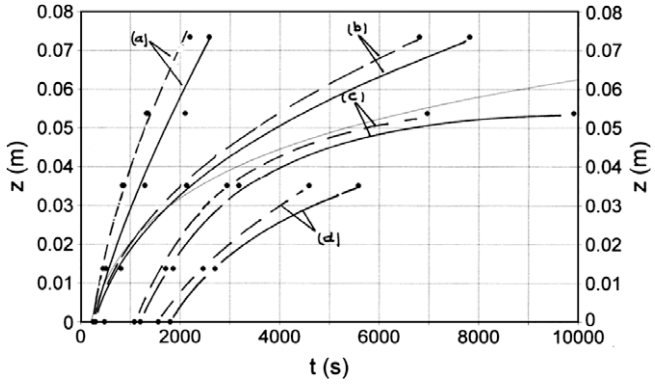

Fig. 13. (a) 25 °C, (b) 30 °C, (c) 43 °C, (d) 50 °C for DS (dash line) and W (continuous line).

- The thermal response to unsteady heating process for all the porous media studied is characterised by the state surface temperature field $T(z,t)$ as it is shown in Fig. 2, and also by $T_p(t)$, $W_{ac}(t)$, and $W_{rf}(t)$ in accordance with Fig. 12.
- The temperature field $T(z,t)$ cannot be fitted with an only equation because it is a three scale problem, even near to the equilibrium state. The effects of contact conductance at both boundaries, hot plate–porous medium and porous medium–refrigeration wall are evident and heat transfer is non-Fourier.
- Experimental results show that whenever the accumulated heat into the porous medium occurs, $W_{ac} > 0$, the lack of LTE is evident. However, provided that the increment of temperature rate is lower than 10^{-4} °C/s, the determination of the thermal conductivity coefficient can be performed applying Price's method and Fourier's law. The difference between the values obtained by both methods is always lower than 8%.
- The thermal conductivity coefficient and the thermal diffusivity depend not only on porous media porosity but also on thermal conductivity of solid matrix and on its structural morphology. Within the knowledge of the authors, no evidence was found in the open technical literature of research work addressing physical models capable to predict the value of these coefficients with enough accuracy.

When the porosity is very great, for instance, the porous medium based on Cotton, the value of the diffusivity is the same order as the saturating liquid. The major causes of lack of LTE are the unsteady characteristic of the heating process and the non-Fourier heat transfer at the boundaries. The first cause is seems evident by analyzing the energy equilibrium in a VER with porosity ε. Let T_0 be the initial equilibrium temperature into the VER, also in equilibrium with its neighbouring. Then, for all temperature variation of one of both phases, the energy equilibrium requires:

$$\varepsilon(\rho C_p)_f \frac{\partial T_f}{\partial t} = (1-\varepsilon)(\rho C_p)\frac{\partial T_s}{\partial t}$$

Therefore, $\dfrac{\partial T_f}{\partial T_s} = \dfrac{(1-\varepsilon)(\rho C_p)_s}{\varepsilon(\rho C_p)_f}$.

Calculating the value of this ratio for the studied porous media we obtain 1.397 (Bronze + W), 0.539 (Sand + W) and 0.0767 (Cotton + W), while at equilibrium state the value must be one. The value of this ratio suggests how much the system is out of equilibrium state and the direction of heat flux at the interface.

The isotherm front propagation velocity depends on the gradient temperature at the interface hot plate–porous medium, and also on the diffusivity value.

The isotherm front propagation velocity is given by the curve slope in each point, and it is diminishing as the distance to the hot plate increases. The addition of a surfactant to the water has a strong influence on the thermal response of porous media. The major effects are:

(i) Lowering the bulk thermal conductivity and diffusivity.
(ii) Lowering the time lag of heat flux and temperature gradient.
(iii) Lowering the contact resistance influence by increased interface wetting.
(iv) Increasing the heat transfer rate into the porous medium and the value of the accumulated heat per time (Fig. 10). This effect is noteworthy in the Cotton + DS porous medium which is due to great affinity between surfactant and cotton, promoting the swelling of the fibres and increasing its active specific surface.

References

[1] International Conference on Porous Media and their Applications in Science, Engineering and Industry, Kona (Hawai), June 1996.
[2] L.X. Xu, J. Liu, Discussion of non-equilibrium heat transfer in biological systems, ASME HTD (1998) 13–17.
[3] R.M. Abalone, M.A. Lara, R. Gaspar, R.D. Piacentivi, Drying of biological products with significant volume variation. Experimental and modelling results for potato drying, Drying Technol. 12 (1994) 629–647.
[4] L. Zhang, P.J. Fryer, Models for the electrical heating of solid–liquid food mixtures, Chem. Eng. Sci. 48 (1993) 633–642.
[5] P.-X. Jicong, M.H. Fau, G.-S. Si, Z. Reu, Thermal hydraulic performance of small scale micro-channels and porous media heat exchanger, Int. J. Heat Mass Transfer 44 (2001) 1039–1051.
[6] K.G.T. Holland, K. Lynkaran, Analytical model for the thermal conductance of compound honeycomb transparent insulation, with experimental validation, Solar Energy 51 (1993) 223–227.
[7] V.A.T. Heek, Increasing the power of high temperature reactor module, Nucl. Eng. Des. 150 (1994) 183–189.
[8] T.C. Chawla, D.R. Pedersen, W.J. Minkowycz, Governing equations for heat and mass transfer in heat generating porous beds. Part I: coolant boiling and transient void propagation, Int. J. Heat Mass Transfer 28 (1985) 2129–2136.
[9] G. Lloyd, K.J. Kim, A. Razurni, K.T. Feldman, Thermal conduction measurement of metal hydride compacts developed for high power reactors, J. Thermophys. Heat Transfer 12 (1) (1998) 132–137.
[10] M.K. Alkam, M.A. Al-Nimr, M.O. Hamdan, Enhancing heat transfer in parallel plate channels by using porous insert, Int. J. Heat Mass Transfer 44 (2001) 931–938.
[11] P. Vadasz, On the paradox of heat conduction in media subject to lack of local thermal equilibrium. A paradox of heat conduction in porous media subject to lack of local thermal equilibrium, Int. J. Heat Mass Transfer 50 (2007) 4131–4140.
[12] D.A. Nield, Effects of local thermal nonequilibrium in steady convection processes in a saturated porous media: forced convection in a channel, J. Porous Media 1 (1998) 181–186.
[13] R.G. Carbonell, S. Whittaker, Heat and mass transfer in porous media, in: J. Bear, M.Y. Corapcioglu (Eds.), Fundamentals of Transport Phenomena in Porous Media, Springer, 1984, pp. 121–198.
[14] A.G. Agwu Nnanrra, A. Haji-Sheikh, K.T. Harris, Experimental study of non-Fourier thermal response in porous media, J. Porous Media 8 (1) (2005) 31–44.
[15] D.A. Nield, A note on the modelling of local thermal non-equilibrium in a structured porous medium, Int. J. Heat Transfer 45 (2002) 4367–4368.

[16] B. Alazmi, K. Vafai, Constant wall heat flux boundary conditions in porous media under local thermal non-equilibrium conditions, Int. J. Heat Mass Transfer 45 (2002) 3071–3087.
[17] G.M. Lloyd, A. Rozani, K.J. Kinn, Formulation and numerical solution of non-local thermal equilibrium equations for multiple gas/solid porous metal hydride reactors, J. Heat Transfer 123 (2001) 520–526.
[18] W.J. Minkowycz, A. Haji-Sheik, K. Vafai, On departure from local thermal equilibrium in porous media due to a rapidly changing heat source: the Sparrow number, Int. J. Heat Mass Transfer 42 (1999) 3373–3385.
[19] G.L. Morini, M. Spige, Transient response of non-thermal equilibrium packed beds, Int. J. Eng. Sci. 37 (1999) 179–188.
[20] A. Maiti, G.D. Mahan, S.T. Pantelides, Dynamical simulation of nonequilibrium processes—heat flow and the Kapitza resistance across grain boundaries, Solid State Commun. 102 (7) (1997) 517–521.
[21] R.J. Stoner, H.J. Maris, Kapitza conductance and heat flow between solids at temperatures from 50 to 300 K, Phys. Rev. B (48) (1993) 16373–16387.
[22] E.T. Swartz, R.D. Pohl, Thermal boundary resistance, Rev. Mod. Phys. 61 (1989) 605–613.
[23] E.T. Swartz, R.D. Pohl, Thermal boundary at interfaces, Appl. Phys. Lett. 51 (1987) 2200–2202.
[24] D.G. Cahill, A. Bullan, S.M. Lee, Interface thermal conductance and the thermal conductivity of multilayer thin films, High Temperature High Press. 32 (2000) 135–142.
[25] J.A. Thomas, A.J.H. McGaughy, Effect of surface wettability on liquid density, structure and diffusion near a solid surface, J. Chem. Phys. 126 (2007).
[26] Kyunil Rah, Byung Chan Eu, Theory of thermal conductivity of dense simple fluids, J. Chem. Phys. 115 (2001) 20.
[27] J.L. Banat, F. Chiaruttini, Mol. Phys. 101 (2003) 1605.
[28] P. Keblinski, J. Themin, Phys. Rev. E 73 (2006).
[29] M. Carbonell, Estudio experimental del proceso de calentamiento de medios porosos saturados hasta ebullición y Dryout de la fase líquida, Ph.D. Thesis, UPC Barcelona, Spain, 1999.
[30] C. Cataneo, A form of heat conduction equation which eliminate the paradox of instantaneous propagation, Compte Rendus 247 (1958) 431–433.
[31] P. Vernotte, Les paradoxes de lu thèorie continue de l'equation de la chaleur, Compte Rendus 246 (1958) 3154–3155.
[32] P. Vernotte, Some possible complications in the phenomena of thermal conduction, Compte Rendus 252 (1961) 2190–2191.
[33] D.Y. Tzon, Macro to microscale heat transfer. The lagging behaviour, in: Series in Chemical and Mechanical Engineering, Taylor & Francis, 1997.
[34] M. Combarnous, S.A. Bories, Modelization de lu convection naturelle an sein d'una couche poreuse horizontale a l'aide d'un coefficient de transfer solid-fluid, Int. J. Heat Mass Transfer 17 (1974) 505–515.
[35] D.Y. Tzon, K.K.S. Chiu, J.E. Beraun, J.K. Chen, Depth of thermal penetration in the fast transient process of heat transport, ASME HTD (1998) 361–364.
[36] S. Kakac, Y. Yener, Heat Conduction, Taylor & Francis, 1993.
[37] O.A. Soboleva, G.A. Badum, B.D. Summ, Absorption of non-ionic surfactant Triton X-100 on solid from aqueous and non-aqueous solutions, Moscow Univ. Chem. Bull. 62 (1) (2007).
[38] G.D. Parfitt, Ch. Rochester, Adsorption from Solution at the Solid/Liquid Interface, Academic, Orlando, 1983.
[39] K. Ofuchi, D. Kunii, Heat transfer characteristics of packed beds with stagnated fluids, Int. J. Heat Mass Transfer 8 (1965) 749–757.